INTERNATIONAL JOURNAL OF CLIMATOLOGY
Int. J. Climatol. (2015)
Published online in Wiley Online Library
(wileyonlinelibrary.com) DOI: 10.1002/joc.4384

RMetS
Royal Meteorological Society

110 years of temperature observations at Orcadas Antarctic Station: multidecadal variability

Miguel E. Zitto,[a,b] Mariana G. Barrucand,[c,d] Rosa Piotrkowski[a,e] and Pablo O. Canziani[b,c]*

[a] *Facultad de Ingeniería, Universidad de Buenos Aires, Ciudad Autónoma de Buenos Aires, Argentina*
[b] *Unidad de Investigación y Desarrollo de las Ingenierías, Facultad Regional Buenos Aires, Universidad Tecnológica Nacional, Ciudad Autónoma de Buenos Aires, Argentina*
[c] *Consejo Nacional de Investigaciones Científicas y Técnicas, CONICET, Argentina*
[d] *DCAO-FCEyN, Universidad de Buenos Aires, Ciudad Autónoma de Buenos Aires, Argentina*
[e] *ECyT, Universidad Nacional de San Martín, San Martín, Prov. de Buenos Aires, Argentina*

ABSTRACT: There is growing evidence of significant changes in components of the Antarctic climate system, an important issue given the influence Antarctica has on global climate. It is important to infer to what extent these regional changes could be attributed to human-induced processes and to what extent to natural variability. Standard methods such as linear trend estimates or piecewise linear trends can be inadequate because they may result in erratic, non-systematic results, particularly if different scales of variability are present in each record and various records are to be compared. The Orcadas Antarctic Station (Argentina), with daily surface meteorological observations since April 1903, provides Antarctica's longest observational record. This study analyses the Orcadas seasonal surface temperature variability. Multidecadal variability and short-term trends are studied to provide an improved assessment of climate evolution and necessary information for the determination of mechanisms driving regional/local change. A combined method using wavelet transform (WT), non-linear statistical model approaches and derivative of fits is developed. This methodology is also applied for validation and comparison to the Gomez ice core oxygen isotope record for the 1857–2006 and 1903–2006 time intervals. Significant quasi 50-year and quasi 20-year variability bands were obtained, both for the quarterly and seasonal Orcadas temperature records, with warming (cooling) periods detected between 1903–1912, 1927–1961 and 1972–2004 (1912–1927 and 1962–1972). If seasons are considered, the only one with a fairly sustained warming is summer, where actual cooling is observed only at the beginning, prior to the early 1930s. Quasi 50-year variability was also detected in the Gomez record. Long periods are obtained in the model fits, longer than the time series, which varied with window length. Although not representing variability cycles, they could represent the best fit of the non-linear, non oscillating asymptotic stationary component of the series, i.e. a non-linear trend.

KEY WORDS Antarctica; climate change; surface temperature; multidecadal variability; wavelet transform; temperature trend

Received 1 October 2014; Revised 23 April 2015; Accepted 24 April 2015

1. Introduction

Antarctica plays a fundamental role in global climate. However, there is growing evidence that significant changes in the components of the Antarctic climate system are taking place. According to IPCC (2013), during the last two decades, both Greenland's and Antarctica's ice covers have lost significant mass. The Intergovernmental Panel on Climate Change (IPCC) assessment concludes that for Antarctica there is a very high confidence level in the observed ice mass losses in the northern part of the Antarctic Peninsula and the Amundsen Sea in West Antarctica. Nevertheless, because of the large uncertainties in the climate observational record, there is low confidence in the attribution of these changes to a human-induced warming in the region.

Much effort has been made to understand temperature trends and change in Antarctica. However, most studies consider the evolution of the Antarctic climate at most since the 1950s, given the limitations in the instrumental records. There is consensus that there is significant warming in the Antarctic Peninsula (Vaughan *et al.*, 2003; Turner *et al.*, 2005; Chapman and Walsh, 2007, among others). Such a strong regional warming may extend into West Antarctica (Steig *et al.*, 2009; O'Donnell *et al.*, 2011). The Antarctic Peninsula warming during austral summer months, in recent decades, has been primarily attributed to the spring ozone 'hole' driving a predominantly positive phase of the Southern Annular Mode (SAM, Thompson and Solomon, 2002; Shindell and Schmidt, 2004; Thompson *et al.*, 2011; WMO, 2011, and references therein). However, there remain some differences among these studies regarding regional and seasonal trends, as well as the overall continental temperature trend.

The main constraint impacting such studies is that almost all instrumental observations in Antarctica as well as at

* Correspondence to: P. O. Canziani, Unidad de Investigación y Desarrollo de las Ingenierías, Facultad Regional Buenos Aires, Universidad Tecnológica Nacional, Av. Medrano 961, C1179AAQ Capital Federal, República Argentina. E-mail: pocanziani@conicet.gov.ar

adjacent locations begin at the earliest in the late 1940s, with a surge in the number of stations during the International Geophysical Year, in 1957, or later. These instruments are mostly located near the continent's coastal areas. Hence, both time and geographical coverage limit the scope for multidecadal variability studies. As noted by some of the abovementioned authors, linear trend estimates suffer from different starting dates of the available records. The shorter the record, the more significant becomes the impact of multidecadal variability on trend estimates. The objective comparison of trends from different sites can, of necessity, only be made during periods when data from the various observation sites overlap, imposing further limitations.

Various attempts have been made to combine ground-based observations with satellite retrievals, reanalysis and/or models, using different techniques to fill in temporal and spatial data gaps (Chapman and Walsh, 2007; Monaghan *et al.*, 2008; Steig *et al.*, 2009; O'Donnell *et al.*, 2011), thus obtaining full coverage of surface temperature fields over Antarctica, but uncertainties remain and the period under study cannot extend back beyond the late 1950s.

Other studies used proxy temperature data from ice cores drilled in different parts of the continent in order to push back the available records to comparatively recent periods in the 18th and 19th centuries, e.g. Schneider *et al.* (2006); Thomas *et al.* (2009); and Thomas *et al.* (2013). Thomas *et al.* (2013) recently noted that the analysis of a 308-year ice core (1702–2009) from Ellsworth Land near the base of the Antarctic Peninsula shows an important warming trend during the last 50–60 years. However, the authors argue that this trend remains within the natural variability of the sample. Steig *et al.* (2013) reached a similar conclusion in a study of West Antarctica. They noted that the current warming trend is similar to previous warming episodes observed in ice cores during the last 2000 years. Thomas *et al.* (2013) point out that such results may not necessarily imply that there is no global warming since, as argued by Karoly and Wu (2005), observational records for about 20% of the Earth's surface do not show 100-year trends that significantly exceed natural variability while the remaining 80% do.

The Orcadas Antarctic Station (60°45′S/44°43′W), managed by the Instituto Antártico Argentino (IAA), has been recording meteorological observations for more than 110 years, with regular daily surface atmospheric monitoring since April 1903. A number of linear trend studies have been carried out with its observations. Skvarca *et al.* (1999) obtained a $-0.4\,^{\circ}\mathrm{C\,decade^{-1}}$ (cooling) linear trend for the period 1904–1930. King *et al.* (2003) and Turner *et al.* (2005), using monthly mean temperature data, obtained a $0.2 \pm 0.1\,^{\circ}\mathrm{C\,decade^{-1}}$ similar overall annual warming trends for the period 1903–2000. Seasonal trends were only slightly different in these studies, clearly overlapping within the error bars. Austral winter (JJA) at Orcadas shows the largest seasonal linear trend for the 20th century, $0.27 \pm 0.24\,^{\circ}\mathrm{C\,decade^{-1}}$, austral summer (DJF) the smallest: $0.15 \pm 0.06\,^{\circ}\mathrm{C\,decade^{-1}}$. Turner *et al.* (2005) considered a sequence of 30-year linear trends obtained with a moving window (displaced 10 years at a time), showing how the Orcadas temperature annual trend varied over time. For the period 1903–1930, they found a trend similar to Skvarca *et al.* (1999), although not statistically significant. While the time series thus analysed exhibited significant trend variability during the 20th century, only the sample's last 30 years have a statistically significant trend at the 90% level: $0.47 \pm 0.57\,^{\circ}\mathrm{C\,decade^{-1}}$. Zazulie *et al.* (2010) analysed the Orcadas daily temperature records' behaviour. They did not find significant change before 1950. When the full sample 1903–2007 was considered, they found a significant warming in the extreme cold days during austral autumn (MAM, $0.53 \pm 0.28\,^{\circ}\mathrm{C\,decade^{-1}}$) and winter ($0.33 \pm 0.20\,^{\circ}\mathrm{C\,decade^{-1}}$), in excess of the mean seasonal warming trend for autumn ($0.42 \pm 0.10\,^{\circ}\mathrm{C\,decade^{-1}}$) and winter ($0.23 \pm 0.15\,^{\circ}\mathrm{C\,decade^{-1}}$). They also found a significant warming trend, since 1970, during summer both in the mean temperature and the daily extremes, which is approximately twice as large as those observed earlier. Zazulie *et al.* (2010) argue that while the warming in summer could in part be due to the spring Antarctic ozone hole (Thompson and Solomon, 2002), the earlier onset of warming during autumn and winter could be due to other processes such as greenhouse gas (GHG) emissions. Thus, different processes could be driving changes in the region (Canziani *et al.*, 2014).

It is an established fact that the time evolution of any meteorological series exhibits a number of different variability scales, from intraseasonal to interdecadal and even centennial periodicities, as well as trends. Such variability, linked to different drivers, internal or external (Sun, volcanoes), masks potential trends. Variability resulting from non-linear interactions in the climate system will further complicate trend estimates. Volcanic eruptions, e.g. El Chichón (1982) and Mt Pinatubo (1991) events, can result in major but short-lived changes in the state of the atmosphere (Compagnucci *et al.*, 2001; Salles *et al.*, 2001; and reference therein). Hence, linear trends, even in a running mean approach (e.g. Turner *et al.*, 2005), include the contributions both of the 'real' trend and multidecadal to centennial variability (cf. the methodological discussion in Huang *et al.*, 1998). It is important to identify the onset of a process leading to a trend change, a non-linear trend or the onset of a climate regime shift, e.g. in 1976–1977 (Ebbesmeyer *et al.*, 1991; Gu and Philander, 1997, among others). All these processes can mask trends, which can thus strongly depend on the beginning and end of the time series, as mentioned above. The challenge is how to deal with non-linear and non-stationary time series.

Identifying and understanding the different scales of variability present in a dataset are thus an important stage in the determination and analysis of change in the climate system. Isolating local or regional scales of variability will contribute towards an improved determination of long-term evolution. Furthermore, determining the regional extent of identified major modes of variability can help understand regional trends even when the

time series available have different starting and ending points. Available methods include standard fast Fourier transform (FFT), empirical orthogonal functions (EOF), wavelet analysis (WT) and empirical mode decomposition method (EMDM), just to mention the more important ones (Huang *et al.*, 1998). Wavelet transform (WT) in particular allows an analysis which provides information not only on the frequencies present in the time series but also the times when the different frequency ranges are present in the sample, thus helping detect non-stationary processes. Moreover, it presents advantages over other methods; it is less restrictive than FFT concerning the local stationarity of the series, leading to results that are more understandable in terms of physical processes. Since Torrence and Compo (1998) introduced the use of wavelets for atmospheric research, the WT has been increasingly used in climate studies (Kumar and Foufoula-Georgiou, 1997; Jevrejeva *et al.*, 2003; Moberg *et al.*, 2005; Barrucand *et al.*, 2008).

This study explores multidecadal variability in the Orcadas surface temperature time series extending from 1903 to 2013. The length and quality of the longest Antarctic time series allow the detection of low frequency variability that can be compared with proxy data. It can be used as a reference to assess the variability of shorter instrumental time series in the vicinity of the Antarctic Peninsula. This analysis proposes the combined use of spectral and statistical model techniques. WT is used as an iterative low-pass filter. The filtered time series is then modelled with sine functions and linear trends using parametric fits. This approach allows the detection of the lower frequency ranges present in the sample, both in amplitude and phase. Furthermore, short-term rates of change of temperature are studied in order to evaluate both the quality of the statistical models and estimate, through a new approach, short-term trend evolution. The results obtained are compared with the results of the analysis applied to the 150-year oxygen isotope record from the Gomez ice core (Thomas *et al.*, 2008, 2009) and previous studies using the Orcadas database.

2. Data and methodology

2.1. Data

Orcadas surface data retrievals (temperature and pressure since 1903, surface winds since 1956) are available online (http://www.antarctica.ac.uk/met/READER/, http://climexp.knmi.nl/). Despite the fact that some months do not have all the daily records, the minimum daily availability is on average more than 95% with exceptional lows of 72–75%. Zazulie *et al.* (2010) show that the Orcadas instrumental record does not present consistency or homogeneity problems throughout the record. This analysis uses monthly mean temperature retrievals for the period 1903–2013.

Figure 1 shows the Orcadas annual temperature cycle and the trend for the period 1903–2013. Minimum temperatures are reached in July ($-10.7 \pm 3.3\,^{\circ}$C) and maxima in February ($0.8 \pm 0.9\,^{\circ}$C). The largest interannual variability is observed during winter months (JJA). The autumn temperature transition is more pronounced than the spring warming. The deseasonalized annual trend over the 111 years of data is $0.20 \pm 0.04\,^{\circ}$C decade^{-1} (95% confidence level, $R^2 = 0.16$). King *et al.* (2003) find a similar trend, $0.20 \pm 0.10\,^{\circ}$C decade^{-1} (95% confidence level) for the period 1903–2000, i.e. the interannual temperature variability during the last 14 years does not appear to have significantly affected the trend.

The Gomez ice core was drilled in 2007 in southwestern Antarctic Peninsula (73.59°S, 70.36°W) near the base of the Antarctic Peninsula, on the western side and with a considerable altitude difference (1400 m) with respect to Orcadas. The oxygen isotope δ^{18}O annual average records are available for the period 1856–2005 (http://www.ncdc.noaa.gov/paleo/icecore/antarctica/gomez/gomez.html). As Thomas *et al.* (2009) note, there is a linear relationship between the isotope's concentration and temperature which is commonly used to infer surface temperatures. Hence, oxygen isotope variability is representative of temperature variability. Figure 2 shows the Gomez oxygen isotope time series together with the Orcadas mean annual temperature record. The longer isotope time series allows (1) the testing of the methodology presented in this paper and its limits and (2) the detection of regional scale variability. Finding similar variability scales in two datasets, from the same region, with completely independent sources of information can further validate the results obtained in this study. It has to be noted that on interannual scales the agreement between Gomez oxygen isotope record and the Orcadas temperature is not very good. However, such scale of variability is not included in the present analysis, which as previously stated, focuses on mutidecadal scales

2.2. Analysis methods

A primary objective of the paper is to present and validate a methodology suited to detect low frequency variability, in this case in the Orcadas temperature series. In consequence, methodology details are now provided.

2.2.1. Continuous WT

The WT is widely used to analyse time series that contain non-stationary power at different frequencies; it provides a time–frequency representation of a signal in the time domain (Mallat, 2008). WTs have been used in geophysical and climatological studies for representation or characterization of such processes (Kumar and Foufoula-Georgiou, 1997; Torrence and Compo, 1998).

The continuous wavelet transform (CWT) of a function $f(t)$ is defined as the integral transformation:

$$(Wf)(s,b) = \int_{-\infty}^{\infty} f(t)\,\overline{\psi_{s,b}(t)}\mathrm{d}t, s \neq 0 \qquad (1)$$

with $\psi_{s,b}(t)$ the 'mother wavelet' $\psi(t)$ dilated by a factor s and translated in b:

$$\psi_{s,b}(t) = \frac{1}{\sqrt{|s|}}\psi\left(\frac{t-b}{s}\right) \qquad (2)$$

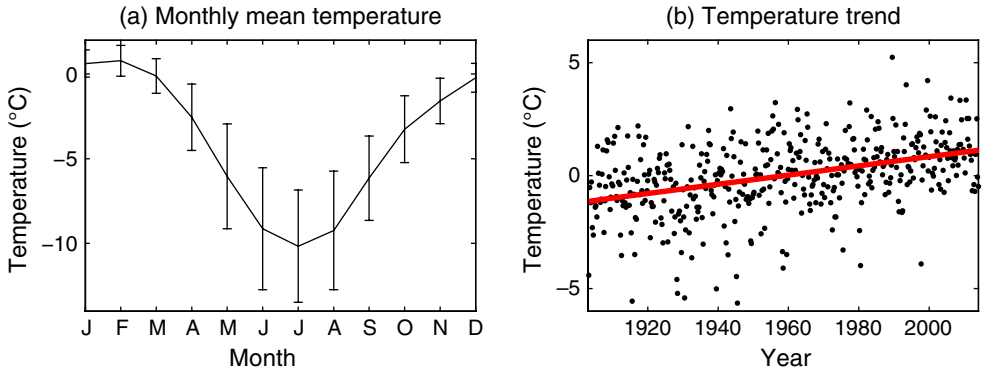

Figure 1. (a) Monthly mean temperature and standard deviation (1903–2013). (b)Temperature anomalies trend for quarterly data; slope = 0.20 ± 0.04 °C decade^{-1} (95% confidence level).

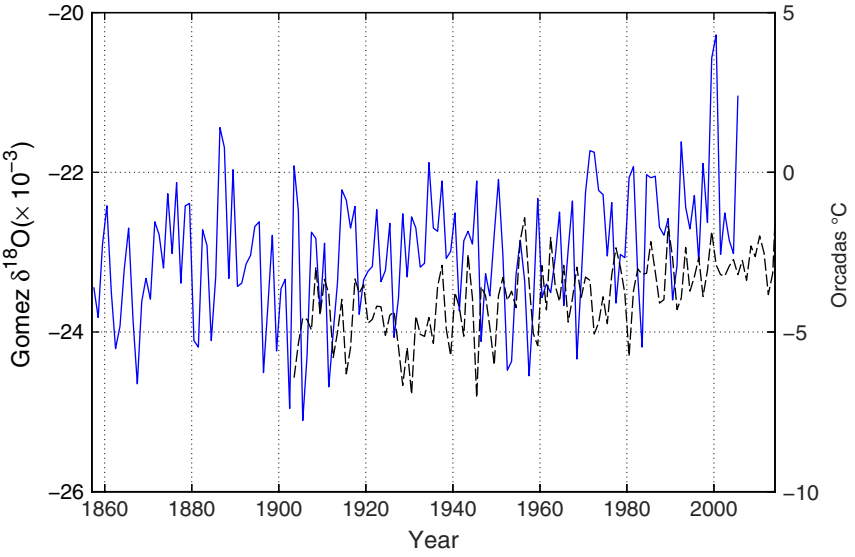

Figure 2. Comparison of the Orcadas annual mean temperature evolution (1903–2013, dashed line) with the Gomez ice core oxygen isotope record (1857–2006, solid line).

In order that $\psi(t)$ be 'admissible' as a wavelet, this function must have a zero mean value and be localized both in time and frequency spaces. The choice of mother wavelet depends on the characteristics of the signal and the kind of information to be extracted. The complex Paul wavelet is particularly suitable for capturing the tendency of a series (Pišoft *et al.*, 2004), whereas the complex Morlet wavelet has a better frequency resolution and thus is very useful to study the general oscillatory characteristics of a series. Equations (3) and (4) give the formulas for the Morlet wavelet and the k-order Paul wavelet, respectively:

$$\psi(\eta) = \pi^{-1/4} e^{ik\eta} e^{-\eta^2/2} \tag{3}$$

$$\psi(\eta) = \frac{2^k i^k k!}{\sqrt{\pi (2k)!}} (1 - i\eta)^{-(k+1)} \tag{4}$$

Figure 3 shows the graph in the time domain, in the frequency domain and the wavelet power spectrum of the Orcadas quarterly (four points – seasonal averages – per year) temperature series for the Morlet and Paul wavelets, respectively.

The CWT of a discrete sequence $x(n\delta t)$ is defined as the convolution of $x(n\delta t)$ with a scaled and translated version of $\psi(t)$ given by:

$$(Wx)(s,n) = \sum_{m=0}^{N-1} x(m\delta t)\, \psi\left[\frac{\overline{(m-n)\,\delta t}}{s}\right] \tag{5}$$

Although it is possible to calculate the WT using these equations, it is considerably faster to calculate in the Fourier space using a discrete Fourier transform (DFT).

2.2.2. *Choices of scales*

It is necessary to choose a set of scales in Equation (5). For non-orthogonal wavelets (such as Morlet or Paul wavelets), one can take an arbitrary set of scales and it is convenient to write the scales as fractional powers of 2,

$$s_j = s_0 2^{j\delta j}, \qquad j = 0, 1, 2, \ \ldots\ , \ J \tag{6}$$

The smaller scale to be resolved, s_0, is generally taken as $s_0 = 2\,\delta t$, and the larger scale corresponding to the index $J = (\delta j)^{-1} log_2(N\delta t/s_0)$ is $s_J = N\delta t$. The value of δj

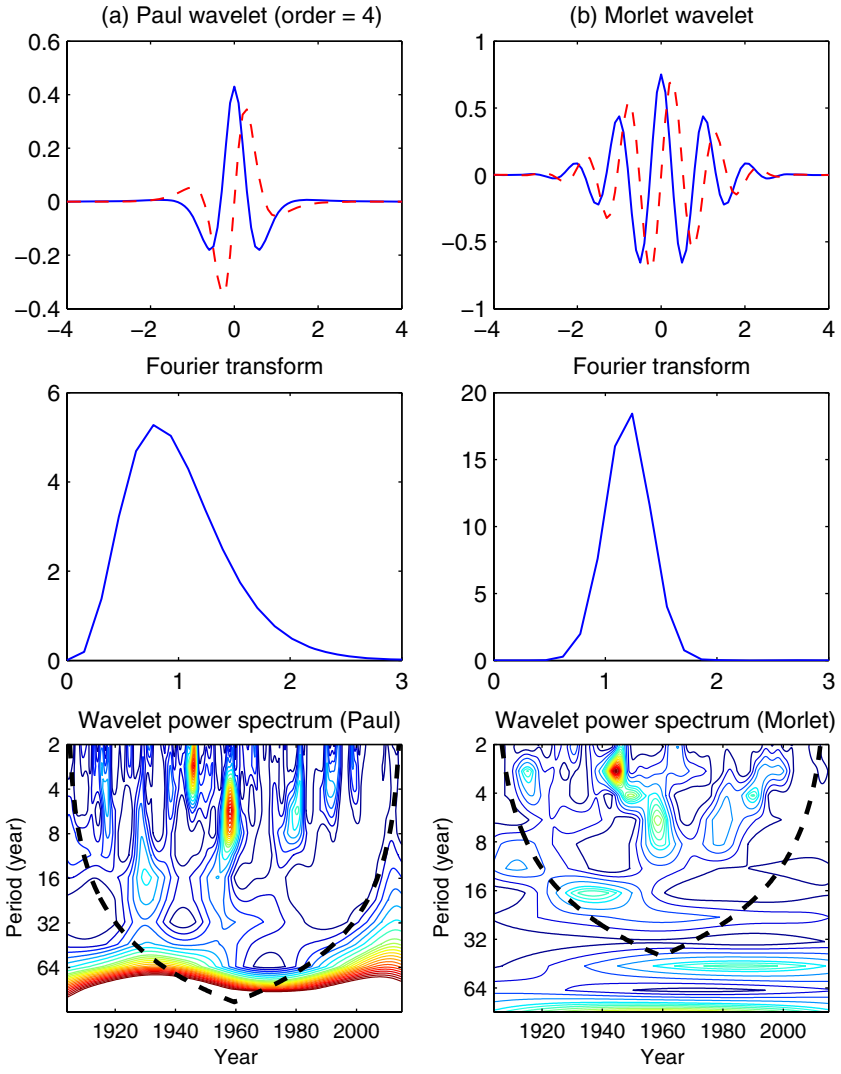

Figure 3. Mother wavelet (a) Paul, (b) Morlet. Top, the real part (solid) and the imaginary part (dashed) for the wavelets in the time domain. Middle, the corresponding absolute values of the Fourier transform. Bottom, wavelet power spectrum for quarterly deseasonalized Orcadas temperature data.

determines the scale resolution; a smaller δj determines a finer resolution. In our work, we selected $\delta j = 0.5$.

2.2.3. *Wavelet power spectrum*

The wavelet function and the WT are both complex. The wavelet power spectrum is defined as $|(Wx)(s,n)|^2$. The power spectra obtained with Morlet and Paul wavelets is shown in Figure 3 (bottom). Similar features can be appreciated in the graphs, but the shape of the Paul wavelet permits to better detect the increment and decrement of a series, for this reason, it is better suited to detect tendencies.

2.2.4. *Reconstruction*

It is possible to reconstruct the original time series from the CWT. This is straightforward for an orthogonal WT, although it is more complicated for the CWT because of the redundancy in time and scale. Yet redundancy has the advantage of allowing the reconstruction of the time series in different scale bands using a completely different wavelet function, the simplest of which is a delta function. For a real time series

$$x_n = \frac{\delta j \delta t^{1/2}}{C_\delta \psi(0)} \sum_{j=0}^{J} \frac{\mathbf{R}\left\{(Wx)\left(s_j, n\right)\right\}}{s_j^{1/2}} \tag{7}$$

where $\mathbf{R}$ is the real part, and index j corresponds to the scale $s_j = s_0\, 2^{(j-1)\delta j}$, with $j = 1,2, \ldots, J$. Factor C_δ comes from the reconstruction of a δ function from its WT using function $\psi(\eta)$. This factor is constant and different for each wavelet function; $C_\delta = 1.132$ for the Paul wavelet and $C_\delta = 0.776$ for the Morlet wavelet.

2.2.5. *Cone of influence*

Because one deals with finite-length time series, errors will occur at the beginning and end of the wavelet power spectrum. Here, the time series is padded with sufficient zeroes to bring the total length N up to the next-higher power of two. Padding with zeroes introduces discontinuities at the endpoints and, as one goes to larger scales, decreases the amplitude near the edges as more zeroes enter the analysis.

The cone of influence (COI) is the region of the wavelet spectrum in which edge effects become important and is defined here as the e-folding time for the autocorrelation of wavelet power at each scale. Figure 3 (bottom row) shows the COI with dashed lines. For power spectra obtained with the Paul wavelet, edge effects are narrower allowing for a broader region within the COI boundaries than for the Morlet one.

2.2.6. Determination of low frequency variability and linear trends

To study the behaviour at low frequencies and potential trends in the Orcadas temperature series, a WT is first applied. A cut-off period P_c can be selected in terms of the observed periods in the wavelet power spectrum and physical considerations. A time series is then reconstructed, as previously described, for periods shorter than P_c. Then the difference between the original and the reconstructed series is calculated, yielding a time series which only contains the longest periods of variability present in the raw data. This difference series between the original raw series and its partial reconstruction does not contain frequencies higher than those corresponding to P_c, the resulting series then is a filtered version of the original signal. The filtered time series is called the residual time series (RTS). Different RTS can be obtained for different P_c values. An iterative smoothing process ends when the original series is reduced to one complete oscillation spanning the series (Pišoft *et al.*, 2004).

When choosing $P_{c,}$ it is important to select a cut-off period that does not have any statistically significant peaks, otherwise spurious variability may arise in RTS. At the same time, it is not convenient to choose a large cut-off period because the larger the period, the narrower the COI becomes, effectively limiting the time span of the RTS. Physical criteria include the need to filter out well-established and higher frequency non-stationary modes of variability in order to facilitate the detection of the longer periods of interest, in this study multidecadal periods.

3. Results

As noted above, the wavelet power spectrum provides information on the convolution between the sampling wavelet at a given scale and the time series at given time interval. Figure 3 (bottom row) shows that for the Orcadas temperature record, applying both the Paul and Morlet wavelets to quarterly mean temperature values yields broad spectral features that are consistent for both wavelets. Inspection of the plots confirms that the Morlet wavelet provides a better frequency resolution while the Paul wavelet provides a better temporal localization of the variability in the different period ranges. The Paul wavelet results in a broader COI. Hence, the Paul wavelet power spectra are used in the present study to obtain the RTS for low frequency detection and analysis.

Figure 4 shows the RTS calculated for different cut-off P_c (11.2; 18.8; 26.6 and 31.6 years, respectively) applied to Orcadas mean quarterly temperature observations, from now on the quarterly series. In order to highlight the low frequency variability, the plots were smoothed with a 9-point running mean to remove the highest frequency variability (periods less than two years) which are too noisy for wavelet sampling. To avoid introducing statistical artefacts and information loss, such filtering was not carried out prior to the wavelet filtering. For all four P_c values, RTS shows overall decreasing temperatures from 1903 till around 1930, followed by temperature increases at least up to 2000.

3.1. Multidecadal variability

The low frequency analysis is carried out using the 18.8 year P_c in order to retain multidecadal variability. While all the P_c values shown above yield similar characteristics, the 18.8-year cut-off period allows for a better detection of the longer period variability present in RTS. Both quarterly (Figure 5) and seasonal (1 point per year, Figure 6) time series were filtered with this P_c. A similar smoothing, using the 9-point moving average, was carried out for all the time series.

The variability in RTS is then analysed using statistical models with two different combinations of sine and linear functions, given the observed nature of the time series. Model M1 is obtained using three sine functions while model M2 considers two sine functions together with a linear one (linear trend). In the particular case of summer, a different model M3 was necessary in order to obtain a statistically significant fit, i.e. two sine functions and a constant. The choice of such statistical models with a limited number of functions was initially based on the visual inspection of the time series which suggested that approach would be sufficient. The results of the fit showed that these were optimal fits to the time series: the final number of functions included in each model was selected in terms of the best significant fit obtained after which the inclusion of additional functions did not result in a significant improvement.

The M1 model for the summer series did not yield a statistically significant fit and when the M2 model was applied to this series, the slope of the linear function was null within the confidence level. The sine functions' amplitudes, frequencies and phases as well as the slope for the linear function were estimated by parameters fitting with the non-linear least-square method (Bates and Watts, 1988). This method allows parameter estimation by minimizing the sum of the squared differences between the modelling functions and the observations. The proposed models are non-linear functions of the parameters, and then minimization is achieved by numerical calculation.

Table 1 shows the results for the relevant parameters (period, amplitude and slope) together with the correlation coefficient. Confidence intervals are shown for the 95% confidence level. From a practical perspective, frequency rather than period was used for the fits given that

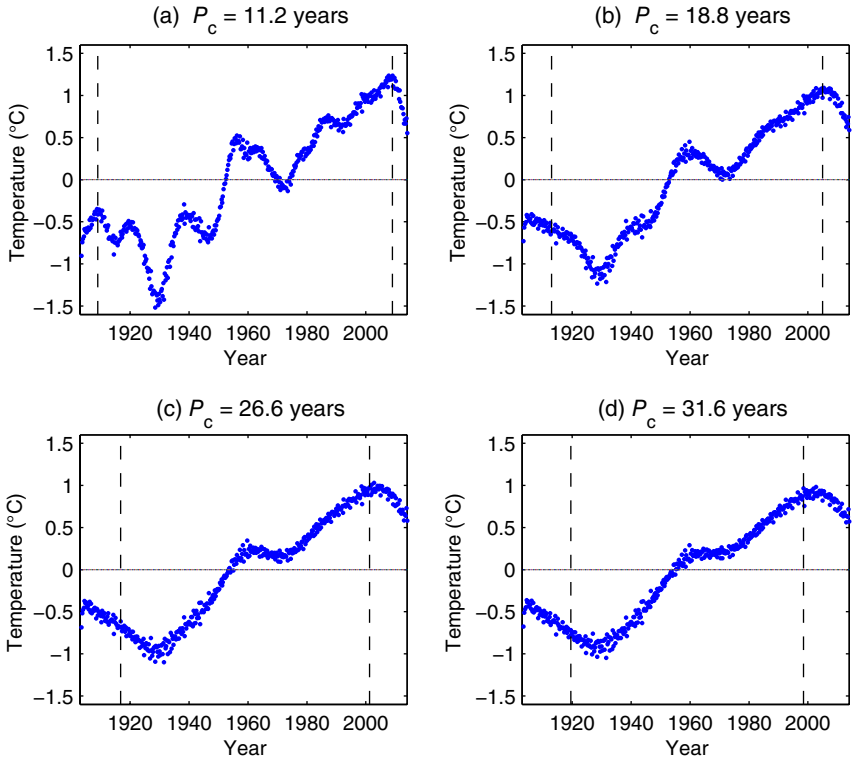

Figure 4. Residual mean quarterly temperature time series (RTS) filtered with different P_c values. Vertical dashed lines show the COI boundaries.

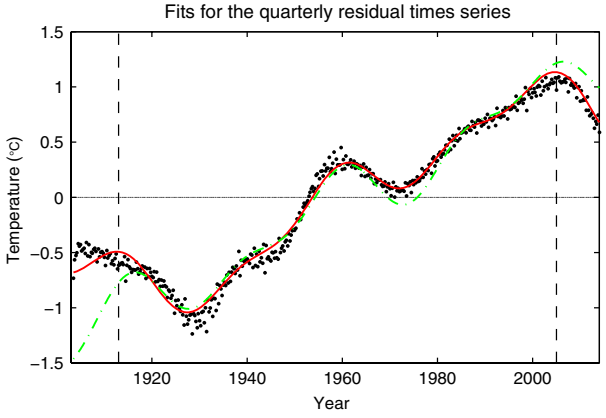

Figure 5. Quarterly residual series (RTS) smoothed with a 9-point moving average (dots). Solid line: fit with model M1. Dashed line: fit with model M2. Vertical dashed lines show COI boundaries.

the calculation process is simpler. The periods shown are straightforwardly derived from the frequency fits. The confidence interval for the periods in consequence is larger as the period increases. When calculating confidence bounds for parameters at a given confidence level, one supposes that the parameter estimators asymptotically follow a normal distribution. The covariance matrix is calculated at the estimated parameter values by means of the Student's t distribution (Huet, 2004).

The quality of the fit is similar for models M1 and M2. M1, with significant R^2 values (cf. Table 1) for quarterly, autumn, winter and spring time series. These fits result in large amplitude, very long period oscillations, spanning from 173 years, in the quarterly sample, to 277 years in the autumn sample. These exceed the sample length, and thus cannot be considered as centennial scale oscillations in the context of dynamical processes. Rather, they are fitting parameters. The second sine function, with periods between 38 and 55 years, has amplitudes which are 30–50% of the previous one. The third sine function, with periods between 22 and 26 years, has amplitudes which are approximately 13–19% of the first sine function. The second sine function will be referred to as quasi 50-year and the third as quasi 20-year period oscillations. The quasi 20-year oscillation is particularly strong and is present throughout the autumn series, while the quasi 50-year one is strongest in winter and spring.

Model M2, for which the very long period oscillation is replaced with a linear function, also results in multidecadal oscillations with periods similar to model M1, i.e. quasi 50-year and quasi 20-year oscillations. The linear function in this model resulted in annual and seasonal long-term trends between 0.021 and 0.029 °C year^{-1}, i.e. spring and winter trends, respectively. These long-term trends are in close agreement with the results obtained by King *et al.* (2003) and Turner *et al.* (2005) using a standard linear trend calculation for the period 1903–2000.

The best summer fit, using the M3 model, yields a 168-year period, again longer than the time series, together with a 21-year oscillation, i.e. quasi 20-years, quasi 50-year being absent. The 20-year period during this season appears to be present primarily during the first half of the sample. Note that in the Morlet power spectrum

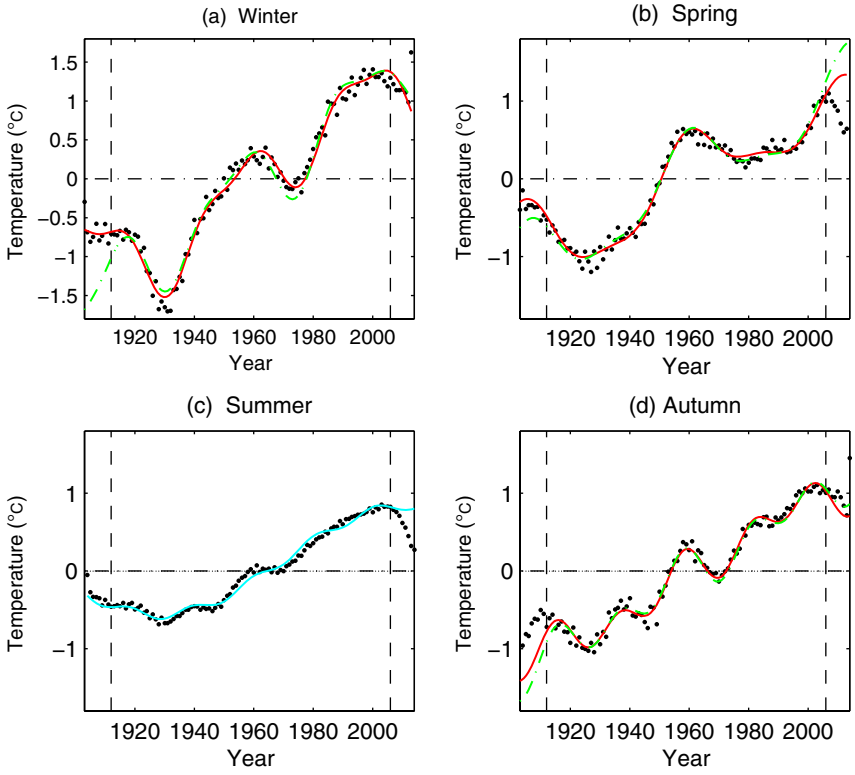

Figure 6. Seasonal residual series (RTS) smoothed with a 9-point moving average (dots): (a) winter, (b) spring, (c) summer and (d) autumn. Solid line: fit with model M1. Dash line: fit with model M2. In the case of summer model, M3 fit is shown by the solid line. Vertical dashed lines show COI boundaries.

Table 1. Non-linear least squares fit parameters for the Orcadas quarterly and seasonal time series.

	Total		Winter		Spring		Summer		Autumn	
	T (year)	A (°C)	T (year)	A (°C)	T (year)	A (°C)	T (year)	A (°C)	T (year)	A (°C)
M1	173 ± 10	0.82 ± 0.03	176 ± 14	1.04 ± 0.04	197 ± 68	0.82 ± 0.13			277 ± 106	1.13 ± 0.25
	46 ± 1	0.24 ± 0.02	45 ± 1	0.44 ± 0.04	55 ± 1	0.43 ± 0.03			38 ± 2	0.44 ± 0.03
	23 ± 1	0.11 ± 0.02	22 ± 1	0.16 ± 0.04	26 ± 1	0.12 ± 0.03			22 ± 1	0.21 ± 0.03
	$R^2 = 0.9883$		$R^2 = 0.9782$		$R^2 = 0.9851$				$R^2 = 0.9858$	
M2	42 ± 1	0.23 ± 0.02	41 ± 1	0.45 ± 0.04	56 ± 2	0.45 ± 0.03			37 ± 2	0.15 ± 0.03
	23 ± 1	0.14 ± 0.02	22 ± 1	0.17 ± 0.04	26 ± 1	0.12 ± 0.03			22 ± 1	0.22 ± 0.03
	$m = (0.023 \pm 0.001)$ °C year^{-1}		$m = (0.029 \pm 0.002)$ °C year^{-1}		$m = (0.021 \pm 0.001)$ °C year^{-1}				$m = (0.023 \pm 0.001)$ °C year^{-1}	
	$R^2 = 0.9792$		$R^2 = 0.9795$		$R^2 = 0.9829$				$R^2 = 0.9837$	
M3							168 ± 13	0.70 ± 0.04		
							21 ± 1	0.05 ± 0.02		
							$R^2 = 0.9872$			

Each sine function is given in terms of T (year), the period in years, and A (°C), the sine amplitude in degrees centigrade for that period.

(Figure 3 bottom row), there is a distinct power maximum near 20 years between 1920 and the early 1950s.

Figures 5 and 6, respectively, show the smoothed quarterly and seasonal RTS and models; the COI is also included in the plots. Note that the M1 model, broadly speaking, results in a better fit throughout the full length of the samples even though all model fits were calculated using observations from within the boundaries of the COI.

The Gomez ice core analysis was carried out with the same procedure, both for the 1857–2006 full sample and the 1903–2006 subset, for comparison with the Orcadas temperature and to evaluate potential windowing issues in the statistical model results. Figures 7 and 8 present the Gomez ice core power spectra and the statistical model results, respectively. Figure 7 shows the Morlet power spectra for the full sample and the 1903–2006 subset. Inspection of both power spectra suggests the presence of 4–8 year oscillations prior to 1920 and after 1950. Despite differences in the sample length in the limit region of the COI, both power spectra exhibit high values between 40- and 64-year periods, extending into the 1990s and a quasi 30-year oscillation prior to 1900. These oscillation bands agree both in period and time of occurrence despite the different sampling periods, showing that these are robust variability features of the Gomez ice core.

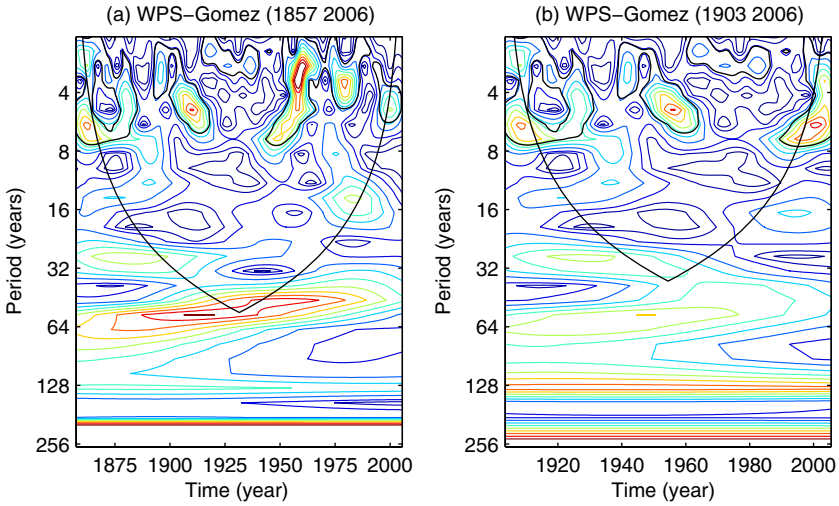

Figure 7. Morlet wavelet spectrum for the Gomez ice core oxygen isotope record (dots): (a) for the full sample 1857–2006 and (b) for the Orcadas observation period overlap 1903–2006.

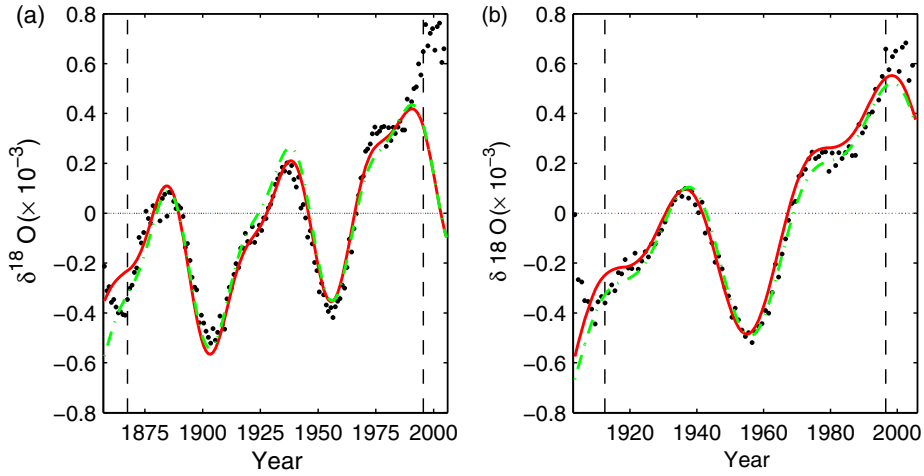

Figure 8. Residual series (RTS) for the Gomez ice core oxygen isotope record (dots): (a) for the full sample 1857–2006 and (b) for the Orcadas observation period overlap 1903–2006. Solid line: fit with model M1. Dash line: fit with model M2.

The statistical model fits (Figure 8) in these cases are optimized with M1 and M2 models as before. For the interval 1857–2006, M1 yielded a 51-, 27- and 253-year oscillations and M2 a 52- and 27-year oscillations (Table 2). For the shorter sample, M2 resulted in 61-, 31- and 3550-year oscillations, while M2 resulted in a 60-year oscillations and 31-year oscillations and a linear trend almost double that of the full sample. The linear trend change agrees with the temporal evolution of the non-linear trend shown in Thomas *et al.* (2009). The larger amplitude short period oscillations always correspond to the quasi 50-year range. This suggests that the quasi 50-year oscillation could be a robust feature throughout the Antarctic Peninsula. However, different periods were obtained in the longer (centennial) scales for the 150-year and the 103-year series. These long period oscillations cannot be attributed to physical oscillations because the periods obtained depend on sample length. As mentioned before, they are fitting parameters.

3.2. A perspective on short-term trends

As previously noted, intercomparison of linear trends between different time series of various lengths, with partial temporal overlaps, remains a significant issue effectively limiting current assessment of local to regional climate processes evolution. Different approaches, including stepwise analyses, have been used (Lanzante *et al.*, 2003; Malanca *et al.*, 2005; Turner *et al.*, 2005) in order to estimate changes in the trends within a given atmospheric time series.

Another option is the 'short term' rate of change, calculated with the derivative of a model fit or with an estimate of the tangent along any point of RTS. It can be used within a given time series to estimate when trends change in sign (turning points) or climate shifts occur as well as to infer short-term linear tendencies, which could help improve our understanding on evolving climate. Given that such short-term rates of change are time dependent, various time series spanning different partially overlapping sampling

Table 2. Non-linear least squares fit parameters for the Gomez ice core oxygen isotope and annual time series.

	Gomez (1857–2006)		Gomez (1903–2006)	
	T (year)	δ^{18}O‰	T (year)	δ^{18}O‰
M1	253 ± 30	0.23 ± 0.02	3550*	4.28*
	51 ± 1	0.28 ± 0.02	61 ± 4	0.29 ± 0.02
	27 ± 1	0.11 ± 0.02	31 ± 1	0.15 ± 0.02
	$R^2 = 0.9467$		$R^2 = 0.9846$	
M2	52 ± 1	0.23 ± 0.02	60 ± 3	0.29 ± 0.02
	27 ± 1	0.14 ± 0.02	31 ± 1	0.15 ± 0.02
	$m = (40 \pm 4) \times 10^{-4}$ δ^{18} O‰/year		$m = (73 \pm 5) \times 10^{-4}$ δ^{18} O‰/year	
	$R^2 = 0.9331$		$R^2 = 0.9866$	

Each sine function is given in terms of T (year), the period in years, and δ^{18}O‰ the sine amplitude for periods 1857–2006 and 1903–2006. *The amplitude of the confidence interval is extremely high at a 95% confidence limit, although there is a good agreement in the graph.

periods can be better compared using these values. This can contribute to the understanding of the temporal and spatial scales of observed multiple time series variability. If two or more series, from different monitoring sites in a given region, of different lengths show similar behaviour during overlapping periods, this could signal that over the span of the longest available time series the regional evolution is similar or coherent at the sites being considered.

Given the good quality of the fits obtained, the trend evolution of the Orcadas temperature is studied in more detail using the analytic derivative of the statistical models (M1, M2 and M3), compared with the numerical differentiation of RTS, to estimate short-term rates of change. The latter differentiation is used as the reference for model results. Such derivatives provide an estimate of the short-term rate of change, at any given time within the sample. This comparison allows further evaluation of the quality of the fits obtained for the RTS.

The numerical differentiation was calculated for the RTS obtained with $P_c = 18.8$ years, as follows:

$$y'\left(t_i\right) = \frac{y\left(t_i + \frac{k\Delta t}{2}\right) - y\left(t_i - \frac{k\Delta t}{2}\right)}{k\Delta t} \tag{8}$$

with $\Delta t = 0.25$ years in the case of quarterly time series, $\Delta t = 1$ year in the case of seasonal time series and $k = 5$.

In order to reduce the noise level and random variations, two points, separated by an interval greater than two years, were selected for the differentiation, hence the k value was defined. It was found that the results did not change much for differentiation intervals somewhat greater than 2 years. Any noise and random variability remaining in the differentiated time series were smoothed with 10- or 20-point moving averages.

Figure 9 shows the smoothed residual quarterly series differentiation (with 20-point smoothing) overlaid with the M1 and M2 analytic derivatives. The period available within the COI was somewhat shortened given the additional intervals required for numerical differentiation. Within the COI boundaries, the derivatives of both models are in good agreement, both in amplitude and phase, with the data differentiation, particularly after 1950. Correlations between the numerical differentiation and the analytic derivatives are good, with the best correlation for M1 being $R^2 = 0.810$, $R^2 = 0.770$ for M2. The largest differences are found prior to 1930. The largest short-term positive rates of change (warming) occur both in data and models in the 1930s and 1950s with peak values close to 0.1 °C year^{-1}. Peak short-term rates of change values in the late 1970s and 1990s are close to 0.05 °C year^{-1}. Positive rate periods (warming) extend from the late 1920s through 1960 approximately, and from the early 1970s through till about 2005, although the latter is beyond the COI boundary. Note that outside the COI model M1 remains somewhat better than M2. Thus, the overall quarterly warming rate at Orcadas appears to have been larger during the first half of the 20th century than during the second half.

Figure 10 shows the numerical differentiation and the analytic derivatives for the residual seasonal series (M1 and M2 for autumn, winter and spring, M3 for summer). In general, within the COI boundaries, there is good agreement between the differentiation and model derivatives. In the case of M1 models, R^2 values with respect to the numerical differentiation series are somewhat better than M2 models in all cases, with values around 0.7. Summer M3 yielded the poorest correlation, with $R^2 = 0.5$.

The largest short-term rate of change occurred during winter with peak values of the order of or greater than 0.1 °C year^{-1}, both positive and negative. Positive maxima (warming) occur during the 1930s and 1970s while negative peak rates of change (cooling) occur during the 1920s and 1960s, i.e. with two similar periods of variability spanning approximately 50-years each, present in both model derivatives. A similar behaviour is found during spring, i.e. a repetitive pattern of variability spanning approximately 50 years, albeit somewhat decreasing in amplitude over time. Autumn shows a strong contribution from quasi 20-year variability. While the overall pattern of variability is similar to the winter one, the stronger presence of the quasi 20-year rate of change results in more frequent, albeit asymmetric, periods of warming and cooling. The evolution during the summer months is dominated, as previously noted, by the quasi 20-year oscillations. This results in a weak (under 0.05 °C year^{-1}) almost continuous positive (warming) rate of change extending from the 1930s through 2000 approximately. The M3 fit after 1970 is poor since the 20-year period vanishes in the observations.

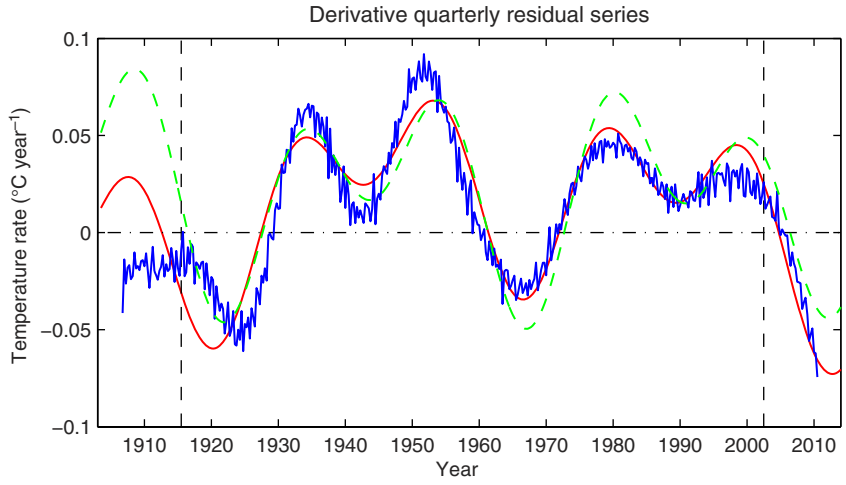

Figure 9. Numerical differentiation of the residual quarterly time series (thin solid line) and the corresponding analytic derivatives for models M1 (solid line) and M2 (dashed line). Thin vertical dashed lines show the COI boundaries.

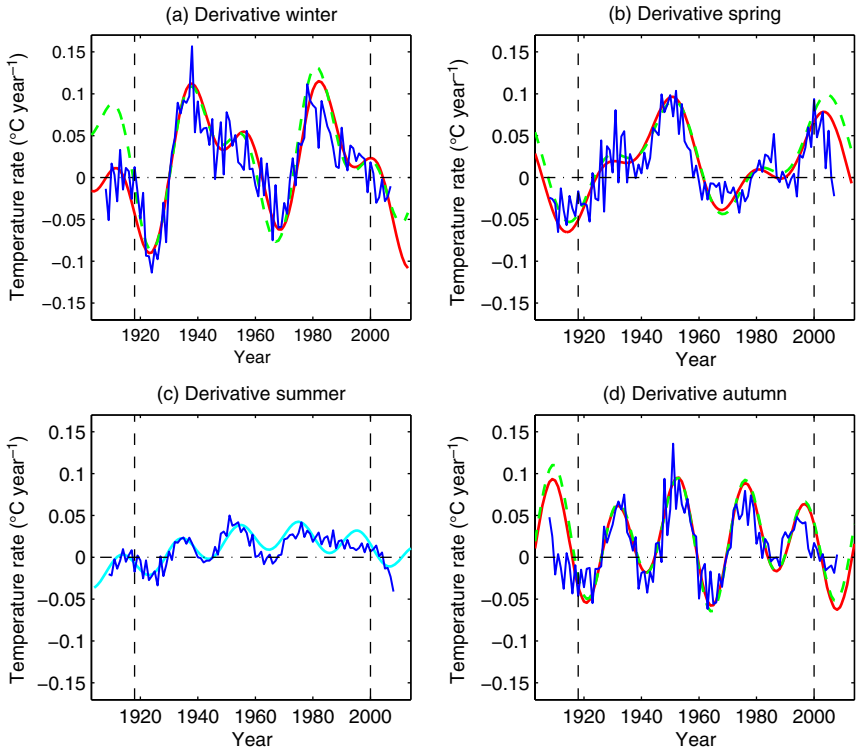

Figure 10. Seasonal numerical differentiation (thin solid line) of residual seasonal time series and the corresponding M1 (solid line), M2 (dashed line) and M3 (solid line-only for summer) analytic derivatives for (a) winter, (b) spring, (c) summer and (d) autumn

4. Discussion

The fact that the statistical models M1, M2 and M3 and their derivatives provide a good representation of both RTS and its differentiation shows that the sum of the proposed functions, with the optimal parameter fits, suitably reflect the low frequency temporal evolution of the Orcadas temperature during the 20th Century. The same can be said of models obtained for the Gomez ice core oxygen isotope data over a longer period. The wavelet analysis demonstrates the non-stationary nature of both time series. The non-linear statistical model fits to the RTS, where the high frequency and highly non-stationary components were removed, highlight some of the low frequency aspects of the time series. It is important to acknowledge that, as for any geophysical process, the Orcadas temperature time series is the result of complex processes, largely stochastic in nature. According to stochastic processes theory, the Karhunen–Loéve theorem (Karhunen, 1947; Loève, 1978) establishes that a stochastic process is represented by a linear combination of an infinite number of orthogonal functions, whose coefficients are random variables and the basis depends on the process being considered. The

orthogonal functions basis to be used in the process's representation is determined by the process's covariance function. It then is a highly valuable fact that with the wavelet filtering here applied in order to remove higher frequency variability in the samples, such good results were obtained when fitting with a sum of three functions.

Present results point to the existence of specific bands of variability in the multidecadal scale over the Antarctic Peninsula, i.e. the quasi 20-year and the quasi 50-year bands. The quasi 50-year oscillations found in Orcadas, present in the quarterly, autumn, winter and spring series, are in good agreement with the variability found for the Gomez ice core. Thomas *et al.* (2013) found a similar period in their wavelet analysis of the 308-year long ice core Ferrigno sample. It corresponds to glaciers in coastal West Antarctica, near the base of the Antarctic Peninsula and hence it is comparatively close to the Gomez site here considered. They also observed variability with periods approximately between 20 and 30 years towards the end of the 19th century and the beginning of the 20th century, again in agreement with present results. Note that during summer, the quasi 20-year oscillation can be visually observed during the first half of the Orcadas sample and during autumn, throughout the 20th century.

Other studies have also found evidence of quasi 20- and 50-year oscillations at high latitudes in both hemispheres. Chylek *et al.* (2011) found in Arctic ice cores a quasi 20-year variability signal. The 45–85 year band however was not statistically significant in this study. Using long-term runs of two climate models (HadCM3 and GFDL CM2.1), they found that the 20-year variability in the Arctic could be related to the Atlantic Multidecadal Oscillation (AMO). Agosta (2014) found a quasi 20-year oscillation in the summer rainfall of subtropical South America on the lee side of the Andes. Agosta (2014) argued that this scale of variability could be linked to the lunar nodal cycle influence on the amplitude of the solar tides. He found a statistically significant correlation with SST variability in the vicinity of the Malvinas (Falkland) Islands. Latif *et al.* (2013) analysed the multidecadal to centennial variability in the Southern Ocean, using different data sources. i.e. tree ring data from Tasmania, spanning more than a thousand years, to derive summer temperatures, ERSSTvb3 sea surface temperatures and the Kiel Climate Model (KCM). They found distinct centennial oscillations in ERSSTvb3 SST between 50° and 70°S, during the instrumental period. A wavelet analysis of the Tasmania tree ring record found statistically significant periods between 45 and 80 years, and in centennial scales.

Thomas *et al.* (2009) show a non-linear trend which varies along the 150 years of the Gomez ice core isotope record. They applied EMDM (Huang *et al.*, 1998) to calculate it. Such a non-linear trend exhibits a minimum prior to 1900 and a sustained increase along the 20th century. The linear trends calculated with M2 for the same dataset over different intervals also show that the trend has increased during the 20th century. The M1 models yielded very long period oscillations, longer than the sample lengths which,

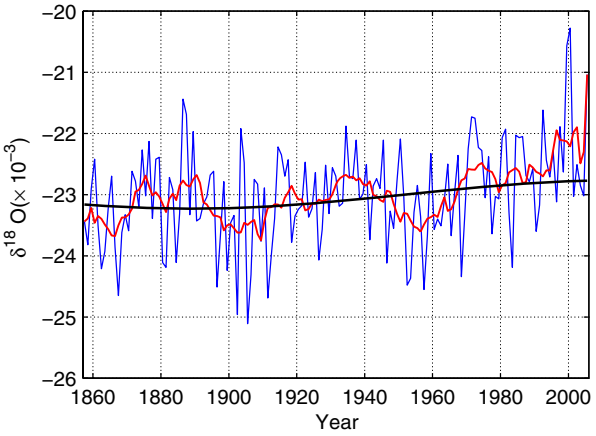

Figure 11. Gomez ice core oxygen isotope record (thin solid line) 1857–2006, overlaid with the 9-point moving average (lighter solid line) and the M1 longest period fit (thick line).

as previously noted, cannot be characterized as real oscillations given their dependency on sample length. However, the M1 models while marginally better within the COI in most cases appeared to better follow the data outside the COI, than M2 models. It could be a sign of the non-linear nature of the trend. The obtained long period sine function is simply optimal in the fitting sense. Figure 11 shows the very long period sine function obtained in the M1 model for the 1857–2006 Gomez ice core time series. Visual comparison with Figure 1 in Thomas *et al.* (2009) permits capturing the similarity between the M1 model and the non-linear trend derived with EMDM.

The shorter the time series are, the more difficult it is to estimate such non-stationary trends. Trends exhibit significant variability on shorter interdecadal timescales. Turner *et al.* (2005) tried to overcome this problem by considering short period linear trend estimates with a sliding window to assess the temporal variability of trends, i.e. using 30-year sampling intervals to estimate short-term trends, displacing this window 10 years at a time to estimate how temperature evolved. Most of these short-term linear trend estimates were non-significant with large standard deviations. Comparison of these trends with the model derivatives and differentiated time series shows that the largest standards deviations coincide with periods where the multidecadal variability enhances temperature change. Hence, for example, for the period 1951–1980, Turner *et al.* (2005) obtain a linear trend $-0.21 \pm 0.84\,^{\circ}\mathrm{C\,decade}^{-1}$. During the same period, the trend estimate from the derivative spans the range -0.3 to $0.9\,^{\circ}\mathrm{C\,decade}^{-1}$ (Figure 9). Furthermore, the trend sign changes twice during this period.

Hence, a sliding window approach, through cancellation of short-term rates of different sign, could erroneously suggest that not much was happening at a given interval, in terms of cooling or warming. Table 3 presents the results of a different approach: the mean trend is calculated between nodes given by null short-term rates of change, for the quarterly time series M1 model. It is thus possible to define periods of sustained warming or cooling,

Table 3. Mean trend calculated between the nodes representing null short-term rates of change for model M1.

Years	Mean trend for model M1 (°C decade^{-1})
1903–1912	0.21 (outside COI)
1912–1927	−0.37
1927–1961	0.40
1961–1972	−0.22
1972–2004	0.32

estimate how long each of them lasts and compare the magnitudes of such warming and cooling intervals. Hence, for the quarterly time series, there appears to have been a warming period between 1903 and 1912 (9 years) followed by cooling between 1912 and 1927 (15 years), and then an extended sustained warming between 1927 and 1961 (34 years). Then a comparatively mild cooling occurred up to 1972 (11 years), and again a sustained warming between 1972 and 2004 (32 years). The latter warming was on average 25% less intense than the longer warming phase spanning the 1930s till 1961. The above analysis also suggests that during the 20th century, the main warming phases at Orcadas lasted somewhat more than 30 years, while the cooling intervals were much shorter, at most 15 years long, and in absolute terms, not as intense.

If the cooling and warming intervals are considered for the seasons, the only one with a fairly sustained warming is summer, where actual cooling is observed only at the beginning, and prior to the early 1930s. For the other seasons, there are distinct periods of cooling, but these also tend to be weaker and short-lived with respect to the warming phases. Any attempt to obtain stepwise trends for these seasons would result in very confusing seasonal 30-year trend estimates.

These results highlight the advantage of considering low frequency variability for trend studies. What would be the criteria to choose the standard averaging window? By what amount should the averaging window be displaced along the time series to capture the main features discussed above? In the case of the Orcadas summer temperature series, 30-year window (the standard climatological averaging interval) spans a period and a half, thus reducing the magnitude of the trend. A 10-year window displacement could systematically additionally reduce the amplitude of the linear trend thus estimated. For the quarterly, autumn, winter and spring series, considering for the time being only quasi 50-year oscillations, a 30-year window would again impact the trend estimate, although the 10-year window displacement would not have as significant an impact on the linear trend. As these series contain both quasi 20-and 50-year oscillations, a 30-year window will result in linear trends and trend variabilities which do not realistically represent the evolution of the sample and may result in the introduction of erratic or non-significant trend estimates. In other words, the appropriate representation of linear trends with moving average requires a choice of averaging window which respects the Nyquist criterion, i.e. the length of the averaging widow has to be shorter than 0.5 the minimum period present in the series and the window displacement a fraction of that minimum period.

Both quarterly and seasonal results show that while warming has prevailed during the 20th century, nevertheless at Orcadas it has not exhibited the largest trends during recent decades, in association with the positive SAM values, driven by the Antarctic ozone hole and GHG increases. According to Thompson and Solomon (2002), the source of the enhanced summer warming in the Antarctic Peninsula and southern Patagonia is the sustained positive SAM index resulting from the spring Antarctic ozone hole. This strong forcing could mask other sources of variability driving, for example, the quasi 20-year oscillation present before 1970. However, this part of the summer sample does not show an enhanced strong warming trend since 1970. Since the 1970s, the warming trend appears to decrease at Orcadas, rather than increase as would be expected from the positive SAM evolution during this period. Legnani *et al.* (2006) found a much larger warming at Orcadas during spring months. Our current analysis also shows that between 1980 and 2000, the warming was more intense during spring than during summer. Marshall (2007) obtained, for the period 1957–2004, non-significant correlations between the Orcadas temperature and SAM during spring and summer. In a follow-up study, Marshall *et al.* (2013) showed that Antarctic surface temperature relationship with SAM can regionally change over time and even reverse sign, i.e. it is not an invariant relationship, most probably as a result of natural variability associated to zonal wave 3. Such results further demonstrate the need for regional long-term variability studies, the intercomparison of various observation sources as well as the development of the best possible long-term climate indices, in order to correctly identify physical coupling and processes involved.

5. Concluding remarks

This study has demonstrated the value of WT analysis combined with statistical modelling to improve the current understanding of long-term climate variability and trends. In particular, the method has been applied to the unique over 110-year long Orcadas Antarctic Station surface temperature record.

Periods in the vicinity of 20 and 50 years were found both in the annual and seasonal time series. Similar periods were found in the Gomez ice core oxygen isotope records for the period 167–2006. These results are in agreement with the recent Thomas *et al.* (2013) study which detected, also using WT 50-year and 20–30-year periodicity in the ice core proxy data. They also found significant but non-continuous variability in the 10–20-year period range. Further comparison with other studies of northern and southern polar and mid-latitude regions, both observational and modelling, highlights the existence of scales of variability with similar time scales to the ones found here. The magnitude of these low frequency temperature

modulations is such that the resulting temperature 'short term' rates of change can be of much larger magnitude than the residual linear trends, as observed both for the quarterly and seasonal time series. The analysis, which obtained results in overall agreement with traditional trend studies over the whole length of the sample, however has highlighted the limitations of trend calculations spanning only a few decades in particular during periods of significant variability.

The linear trends for quarterly and seasonal time series agree with previous studies. As noted, periods of the order of 150–200 years, or even longer, were also obtained in this study, They do not represent physical centennial oscillation scales but rather appear to represent the best long period sine function for data fitting. The model function composed of three sines and was a better representation of the series than two sines with a linear trend. Thomas *et al.* (2009) obtained a non-linear trend function for the Gomez ice core oxygen isotope dataset, using EMDM. The very long period sine fit obtained here reproduced a similar evolution. Hence, these results suggest the need to consider non-linear trends in future studies rather than standard linear trend estimates. Further work is necessary to understand the drivers of the observed variability and to compare current results with similar studies for other sites in the vicinity of the Antarctic Peninsula and Southern South America.

Acknowledgements

The authors wish to acknowledge funding from projects ANPCyT PICT 2012 2927 (Ministerio de Ciencia Tecnología e Innovación Productiva de la Nación) and Program UBACyT 2013–2016, 20020120100340 and UBACyT 2014–2016 20020130200142BA (Universidad de Buenos Aires) and the two anonymous reviewers for their valuable contributions.

References

Agosta E. 2014. The 18.6-year nodal tidal cycle and the bi-decadal precipitation oscillation over the plains to the east of subtropical Andes, South America. *Int. J. Climatol.* **34**: 1606–1614.

Barrucand M, Rusticucci M, Vargas W. 2008. Temperature extremes in the south of South America in relation to Atlantic Ocean surface temperature and Southern Hemisphere circulation. *J. Geophys. Res.* **113**: D20111, doi: 10.1029/2007JD009026.

Bates DM, Watts DG. 1988. *Nonlinear Regression Analysis and Its Applications*. John Wiley and Sons: New York, NY.

Canziani PO, O´Neill A, Schofield R, Raphael M, Marshall GJ, Redaelli G. 2014. World Climate Research Programme Special Workshop on climatic effects of ozone depletion in the Southern Hemisphere. *Bull. Am. Meteorol. Soc.* **95**: ES101–ES105, doi: 10.1175/BAMS-D-13-00143.1.

Chapman W, Walsh J. 2007. A synthesis of Antarctic temperatures. *J. Clim.* **20**: 4096–4117.

Chylek P, Folland CK, Dijkstra HA, Lesins G, Dubey MK. 2011. Ice-core data evidence for a prominent near 20 year time-scale of the Atlantic Multidecadal Oscillation. *Geophys. Res. Lett.* **38**: L13704, doi: 10.1029/2011GL047501.

Compagnucci RH, Salles MA, Canziani PO. 2001. The spatial and temporal behaviour of the lower stratospheric temperature over the Southern Hemisphere: the MSU view. Part I: methodology and temporal behaviour. *Int. J. Climatol.* **21**: 419–437.

Ebbesmeyer CC, Cayan DR, McLain DR, Nichols FH, Peterson DH, Redmond KT. 1991. 1976 step in the Pacific climate: forty environmental changes between 1968–75 and 1977–1984. In *Proceedings of 7th Annual Pacific Climate Workshop*, Asilomar, CA, Interagency Ecological Studies Program Technical Report No. 26, Betancourt JL, Tharp VL (eds). California Department of Water Resources: Sacramento, CA, 115–126.

Gu D, Philander SGH. 1997. Interdecadal climate fluctuations that depend on exchanges between the tropics and extratropics. *Science* **275**: 805–807.

Huang NE, Shen Z, Long SR, Wu MC, Shih HH, Zhen Q, Yen N-C, Tung C-C, Liu HH. 1998. The empirical mode decomposition and the Hilbert spectrum for non linear and non-stationary time series analysis. *Proc. R. Soc. Lond. A* **454**: 903–995.

Huet S (ed). 2004. *Statistical Tools for Nonlinear Regression: A Practical Guide With S-PLUS and R Examples*. Springer Science & Business Media: New York, NY.

IPCC. 2013. *Climate Change 2013: The Physical Science Basis, Working Group I Contribution to the Fifth Assessment Report of the Intergovernmental Panel on Climate Change*. Cambridge University Press: New York, NY. ISBN: 978-1-107-66182-0.

Jevrejeva S, Moore JC, Grinsted A. 2003. Influence of the Arctic Oscillation and El Niño-Southern Oscillation (ENSO) on ice conditions in the Baltic Sea: the wavelet approach. *J. Geophys. Res.* **108**: 4677, doi: 10.1029/2003JD003417.

Karhunen K. 1947. Überlineare Methoden in der Wahrscheinlichkeitsrechnung. *Ann. Acad. Sci. Fennicae. Ser. A. I. Math. Phys.* **37**: 1–79.

Karoly DJ, Wu Q. 2005. Detection of regional surface temperature trends. *J. Clim.* **18**: 4337–4343.

King JC, Turner J, Marshall GJ, Connolley WM, Lachlan-Cope TA. 2003. Antarctic Peninsula climate variability and its causes as revealed by analysis of instrumental records. *Antarctic Res. Ser.* **79**: 17–30.

Kumar P, Foufoula-Georgiou E. 1997. Wavelet analysis for geophysical applications. *Rev. Geophys.* **35**(4): 385–412.

Lanzante JR, Klein SA, Seidel DJ. 2003. Temporal homogenization of monthly radiosonde temperature data. Part II: trends, sensitivities and MSU comparisons. *J. Clim.* **16**: 241–262.

Latif M, Martin T, Park W. 2013. Southern ocean sector centennial climate variability and recent decadal trends. *J. Clim.* **26**(19): 7767–7782.

Legnani W, Canziani P, Barletta J, Gil G, Ibañez F. 2006. 100 years of surface weather observations at Orcadas Antarctic Station: a look at variability and change in the Antarctic Peninsula. In *Proceedings of the 8th International Conference on Southern Hemisphere Meteorology and Oceanography*, INPE, Foz do Iguazu, Brazil, 24–28 April, 195–199.

Loève M. 1978. *Probability Theory*. Graduate Texts in Mathematics 46, Vol. **II**, 4th edn. Springer-Verlag: New York, NY. ISBN: 0-387-90262-7.

Malanca FE, Canziani PO, Argüello G. 2005. Trends evolution of ozone between 1980 and 2000 at mid-latitudes over the Southern Hemisphere: decadal differences in trends. *J. Geophys. Res.* **110**: D05102, doi: 10.1029/2004JD004977.

Mallat S. 2008. *A Wavelet Tour of Signal Processing: The Sparse Way*, 3rd edn. Academic Press: New York, NY. ISBN: 0123743702 9780123743701.

Marshall GJ. 2007. Half-century seasonal relationships between the Southern Annular Mode and Antarctic temperatures. *Int. J. Climatol.* **26**: 373–383.

Marshall GJ, Orr A, Turner J. 2013. A predominant reversal in the relationship between the SAM and East Antarctic temperatures during the twenty-first century. *J. Clim.* **26**: 5196–5204.

Moberg A, Sonechkin DM, Holmgren K, Datsenko NM, Karlén W. 2005. Highly variable Northern Hemisphere temperatures reconstructed from low- and high-resolution proxy data. *Nature* **433**: 613–617.

Monaghan AJ, Bromwich DH, Chapman W, Comiso J. 2008. Recent variability and trends of Antarctic near-surface temperature. *J. Geophys. Res.* **113**: D04105, doi: 10.1029/2007JD009094.

O'Donnell R, Lewis N, Mcintyre S, Condon J. 2011. Improved methods for PCA-based reconstructions: case study using the Steig et al. (2009) antarctic temperature reconstruction. *J. Clim.* **24**: 2099–2115.

Pišoft P, Kalvová J, Brázdil R. 2004. Cycles and trends in the Czech temperature series using wavelet transforms. *Int. J. Climatol.* **24**: 1661–1670.

Salles MA, Canziani P, Compagnucci RH. 2001. The spatial and temporal behaviour of the lower stratospheric temperature over the Southern Hemisphere: the MSU view. Part II: spatial behaviour. *Int. J. Climatol.* **21**: 439–454.

Schneider D, Steig E, van Ommen T, Dixon D, Mayewski P, Jones J, Bitz C. 2006. Antarctic temperatures over the past two centuries from ice cores. *Geophys. Res. Lett.* **33**: L16707, doi: 10.1029/2006GL027057.

Shindell DT, Schmidt GA. 2004. Southern Hemisphere climate response to ozone changes and greenhouse gas increases. *Geophys. Res. Lett.* **31**: L18209, doi: 10.1029/2004GL020724.

Skvarca P, Rack W, Rott H, Ibarzibal y Doningelo T. 1999. Climatic trend and the retreat and disintegration of ice shelves on the Antarctic Peninsula: an overview. *Polar Res.* **18**: 151–157.

Steig EJ, Schneider D, Rutherford SD, Mann ME, Comiso JC, Shindell DT. 2009. Warming of the Antarctic ice-sheet surface since the 1957 International Geophysical Year. *Nature* **457**: 459–462.

Steig E, Ding Q, White J, Küttel M, Rupper S, Neumann T, Neff P, Gallant A, Mayewski P, Taylor K, Hoffmann G, Dixon D, Schoenemann S, Markle B, Fudge T, Schneider D, Schauer A, Teel R, Vaughn B, Burgener L, Williams J, Korotkikh E. 2013. Recent climate and ice-sheet changes in West Antarctica compared with the past 2,000 years. *Nat. Geosci.* **6**: 372–375.

Thomas ER, Marshall G, McConnell JR. 2008. A doubling in accumulation in the western Antarctic Peninsula since 1850. *Geophys. Res. Lett.* **35**: L01706, doi: 10.1029/2007GL032529.

Thomas ER, Dennis P, Bracegirdle T, Franzke C. 2009. Ice core evidence for significant 100-year regional warming on the Antarctic Peninsula. *Geophys. Res. Lett.* **36**: L20704, doi: 10.1029/2009GL040104.

Thomas E, Bracegirdle T, Turner J, Wolff E. 2013. A 308 year record of climate variability in West Antarctica. *Geophys. Res. Lett.* **40**: 5492–5496, doi: 10.1002/2013GL057782.

Thompson DWJ, Solomon S. 2002. Interpretation of recent Southern Hemisphere climate change. *Science* **296**: 895–899.

Thompson DWJ, Solomon S, Kushner PJ, England MH, Grise KM, Karoly DJ. 2011. Signatures of the Antarctic ozone hole in Southern Hemisphere surface climate change. *Nat. Geosci.* **4**: 741–749.

Torrence C, Compo G. 1998. A practical guide to wavelet analysis. *Bull. Am. Meteorol. Soc.* **79**(1): 61–78.

Turner J, Colwell S, Marshall G, Lachlan-Cope T, Carleton A, Jones P, Lagun V, Reid P, Iagovkina S. 2005. Antarctic climate change during the last 50 years. *Int. J. Climatol.* **25**: 279–294.

Vaughan DG, Marshall GJ, Connolley WM, Parkinson C, Mulvaney R, Hodgson DA, King JC, Turner J. 2003. Recent rapid regional climate warming on the Antarctic Peninsula. *Clim. Change* **60**: 243–274.

WMO. 2011. Scientific assessment of ozone depletion: 2010. Global Ozone Research and Monitoring Project Report No. 52, World Meteorological Organization, Geneva, Switzerland.

Zazulie N, Rusticucci M, Solomon S. 2010. Changes in climate at high southern latitudes: a unique daily record at Orcadas spanning 1903–2008. *J. Clim.* **23**: 189–196.

